Biointerface Research in Applied Chemistry
Open-Access Journal (ISSN: 2069-5837)

Article
Volume 13, Issue 4, 2023, 311
https://doi.org/10.33263/BRIAC134.311

Mathematical Modelling of Convective Diffusive Mass Transfer in Ferrofluids Concerning Targeted Drug Delivery

Punit Kumar Deshapande [1], Sravan Kumar Thavada [2,*], Vijaya Kumar Avula Golla [3]

[1] Department of Mathematics, SoAS, REVA University, Bangalore-560064, Karnataka, India; punithkumardn@reva.edu.in (P.K.D.);
[2] Department of Mathematics, Atria Institute of Technology, Bangalore-560024, Karnataka, India; thavadasravankumar@gmail.com (S.K.T.);
[3] Department of Mathematics, SAS, Vellore Institute of Technology, Vellore-632014; vijayakumarag@vit.ac.in (V.K.A.G.);
* Correspondence: thavadasravankumar@gmail.com (S.K.T.);

Scopus Author ID 56872884700
Received: 9.06.2022; Accepted: 8.07.2022; Published: 11.09.2022

Abstract: Magnetically targeted drug delivery systems have been gaining importance over recent years due to their efficiency and minimal side effects. Many techniques are proposed for delivering drugs to targeted sites within the human body. But magnetically targeted drug delivery surpasses because of its unique character and high efficiency. There are only a few theoretical analyses done by researchers addressing the hydrodynamic models of magnetic fluids in the blood vessel. This paper presents a mathematical model of the hydrodynamics of the fluid, blood flow, and convective diffusive mass transfer of the species. Here we have tried to analyze a drug delivery method for delivering a drug to a specific site in the body. For this analysis, we have considered a channel bounded by the tissue region where the drug is targeted. An exact analysis of unsteady convective diffusive solute transfer in a channel bounded by a tissue region under the influence of a magnetic field.

Keywords: magnetic targeting drug delivery; ferrofluids; hydrodynamic modeling; dispersion model.

1. Introduction

Magnetically targeted drug delivery is a method for delivering a drug to a specific site in the body by attaching the drug to small paramagnetic particles (nanoparticles). This compound is injected into the bloodstream, which supplies to the targeted site under an external magnetic field. Magnetic drug targeting therapy can be used for the medical treatment of various diseases like stenosis, thrombosis, and cancer. Handan [1] has considered a blood vessel in the target region where magnetic microspheres are convicted and developed a mathematical model describing the process for a single magnetic particle. The computational fluid dynamics approach is adopted by modeling ferrofluids flow in a blood vessel. Ferrofluids are colloidal solutions of ferromagnetic nanoparticles in a carrier fluid. They need to be bio-degradable to find use in medicine, and certain *in vivo* and *in vitro* experiments have been performed [2-6]. The dispersion behavior in oscillatory flows in uniform conduits is studied using a similar methodology.

Additionally, it is demonstrated that turbulent motion causes heat and other diffusible qualities to diffuse through the fluid's interior [7-9]. Many models have been developed to study nanofluid transportation in bio tissue in the case of magnetic hyperthermia by Tang, Yun-dong *et al*. [10]. Magnetic targeting of the drug under the effect of the applied magnetic field is studied numerically by Sharifi Abbas *et al*. [11]. Innovative models have been developed to study the electro-osmotic flow of Couette nanofluids [12]. A study on the effect of stenosis on magneto nanoparticle distributions in the presence of a magnetic field is presented by Varmazyar *et al*. [13]. Characteristics of various parameters of ferrofluids are studied using numerical and analytical methods by Nadeem *et al*. [14]. Punith Kumar *et al*. [15] studied the effects of convective mass transfer and magnetic field in the case of catheter-based drug delivery. Ismaeel *et al*. [16] reviewed and presented the methods related to nanofluid principles focusing on biofluid mass transfer. Ghulam Rasool *et al*. [17] studied a 2D model of treatment for cancer. The coupled governing equations are defined and solved for nanoparticle flow. Farshad Moradi Kashkooli *et al*. [18] examined the Darcy-Forchheimer relation numerically by considering convective nanofluid flow past a stretching sheet. A uniform magnetic field is applied over the flow, and a small Reynolds number is applied. The numerical solution is obtained for governing problems.

The drug delivery process to tumors in solid form using nano-sized drug delivery systems. Conventional therapy through various stages is compared and simulated. Punith Kumar and Indira [20] reported on various models for drug delivery systems for cancer. They discussed numerical methods and simulation models available for bio-interaction representations in biosystems. Zakaria Korei *et al*. [21] conducted research on lid-driven cavity problems considering MHD flow. Xue-Lin Gao *et al*. [22] studied impacts on heat transfer between solid and liquid. They developed a square cavity model and studied the physical properties. The Boltzmann method is used to solve the defined equations. Sukumar Pati *et al*. [23] critically reviewed forced convective heat transfer through porous media. They provided recommendations on critical areas [24-29] and discussed comparing nanofluids with traditional coolants. This is demonstrated by considering alumina water flow through parallel fins inside a hexagonal boundary.

As earlier work viewpoint cited, the general purpose is the analysis of the behavior of the flow field components; it appears in many studies that deal with the fluid flows through channels. These problems are solved using the Navier-Stokes equations. Still, the difference from one problem to another is related to the constraints associated with the flow and the type of solution sought. Regarding the constraints, it is important to point out that the Navier-Stokes equations are very sensitive to the boundary and initial conditions. This is to say, for example, that the same differential equation can formulate many problems. Still, the difference at the level of the solutions is mainly related to the boundary conditions.

On the other hand, the type of solution sought is related to the method used to solve the problem. This allows us to highlight the particularity of our current study compared to all the previous works cited at this stage. The present model, which includes hydrodynamics of the fluid, blood flow, and convective diffusive mass transfer of the species, is considered, and an analytical solution is obtained. So, this kind of solution has never been reported elsewhere.

2. Materials and Methods

A channel bounded by the tissue region where the drug is targeted considered with an external magnetic field application. Blood acts as a magnetically conducting fluid. A model similar to dusty viscous fluid is used to account for the suspensions that carry the drug.

Assuming fully developed flow (Figure 1), Navier-stokes equations in regions 1 and 2 reduce to

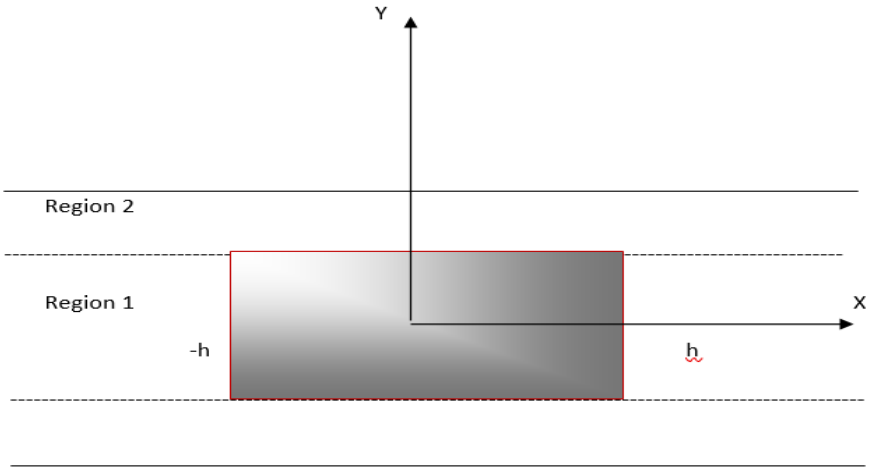

Figure 1. Schematic of physical configuration.

Region 1

$$\rho\frac{\partial u_1}{\partial t}=-\frac{\partial P}{\partial x}+\mu_1\frac{\partial^2 u_1}{\partial y^2}+KN\left(v_1-u_1\right)-\sigma_e B_0^2 u_1 \tag{2.1}$$

$$m\frac{\partial v_1}{\partial t}=K\left(u_1-v_1\right) \tag{2.2}$$

Region 2

$$\rho\frac{\partial u_2}{\partial t}=-\frac{\partial P}{\partial x}+\mu_2\frac{\partial^2 u_2}{\partial y^2}+KN\left(v_2-u_2\right)-\sigma_e B_0^2 u_2-\frac{\mu_2}{K_0}u_2 \tag{2.3}$$

$$m\frac{\partial v_2}{\partial t}=K\left(u_2-v_2\right) \tag{2.4}$$

The boundary conditions are given by

$$\frac{\partial u_1}{\partial t}=0 \qquad at \qquad y=0 \qquad \text{(Symmetry)} \tag{2.5}$$

$$u_1=u_2, \qquad \mu_1\frac{\partial u_1}{\partial y}=\mu_2\frac{\partial u_2}{\partial y} \qquad at \qquad y=h \qquad \text{(Matching)} \tag{2.6}$$

$$u_2=0 \qquad at \qquad y=h_1 \qquad \text{(no-slip)} \tag{2.7}$$

Nondimensionalising using $y^*=\frac{y}{h}$, $u^*=\frac{u_i}{u_0}$, $v^*=\frac{v_i}{v_0}$, and substituting

$u_i=U_i(y)e^{-nt}$, $v_i=V_i(y)e^{-nt}$, $\frac{\partial P}{\partial x}=-P\,e^{-nt}$ we get the equations as

$$\frac{d^2u_1}{dy^2}+w_1^2u_1=-RP \quad \text{in region 1} \quad \text{and} \tag{2.8}$$

$$\frac{d^2u_2}{dy^2}+w_2^2u_2=-R\lambda P \quad \text{in region 2} \tag{2.9}$$

$$\text{where } w_1^2=\left(\frac{KN_1}{\rho}\frac{n\tau}{1-n\tau}+n\right)\frac{\rho h^2}{\mu_1}-\frac{\sigma_e B_1^2 h^2}{\mu_1},\ R=\frac{\rho h^2}{\mu_0\mu_1},V_1=\frac{\mu_1}{1-n\tau},V_2=\frac{\mu_2}{1-n\tau}, \tag{2.10}$$

Boundary conditions after non-dimensionalizing are given by

$$\frac{\partial u_1}{\partial y}=0 \qquad at \qquad y=0 \tag{2.11}$$

$$u_1=u_2,\quad \frac{\partial u_1}{\partial y}=\lambda\frac{\partial u_2}{\partial y} \qquad at \qquad y=1 \tag{2.12}$$

$$u_2=0 \qquad at \qquad y=1+h'$$

Solving (2.8) and (2.9) using (2.10) to (2.12), we get the axial velocity of the convecting fluid i.e 2blood as

$$u_1=RP\left(a_1\cos\omega_1 y-\frac{1}{\omega_1^2}\right) \tag{2.13}$$

$$u_2=RP\left(a_2\cos\omega_2 y+a_1\sin\omega_2 y-\frac{\lambda}{\omega_2^2}\right) \tag{2.14}$$

Where $a_1, a_2 and\ a_3$ are listed in the appendix.

The average velocity over region 1 is given by

$$\bar{u}_1=\int_0^1 u_1dy=RP\left(a_3\frac{\sin\omega_1}{\omega_1}-\frac{1}{\omega_1^2}\right) \tag{2.15}$$

$$\bar{u}_2=\int_0^{1+h'} u_2dy=RP\left(\frac{a_2}{\omega_2}\{\sin\omega_2(1+h')-\sin\omega_2\}-\frac{a_1}{\omega_2}\{\cos\omega_2(1+h')-\cos\omega_2\}-\frac{\lambda h'}{\omega_2^2}\right) \tag{2.16}$$

The particle velocity $V_i(y) for\ i=1,2$ can be obtained from (2) and (4) using the assumption

$$V_i=\frac{u_i(y)}{1-n\tau},\ for\ \ i=1,2 \tag{2.16a}$$

In a drug delivery system, it is necessary to keep track of the concentration of each species. The convective diffusive species equation in both regions is given by

Region 1

$$\frac{\partial C_1}{\partial t}+u_1\frac{\partial C_1}{\partial x}+\frac{KN}{\rho}\left(\frac{\partial C_1}{\partial t}+v_1\frac{\partial C_1}{\partial x}\right)=D_1\left(\frac{\partial^2 C_1}{\partial x^2}+\frac{\partial^2 C_1}{\partial y^2}\right) \tag{2.17}$$

Region 2

$$\frac{\partial C_2}{\partial t}+u_2\frac{\partial C_2}{\partial x}+\frac{KN}{\rho}\left(\frac{\partial C_2}{\partial t}+v_2\frac{\partial C_2}{\partial x}\right)=D_2\left(\frac{\partial^2 C_2}{\partial x^2}+\frac{\partial^2 C_2}{\partial y^2}\right) \tag{2.18}$$

The drug, in the form of a suspension, is mixed with a biocompatible ferrofluid and injected into the blood flow. Due to this, the initial and boundary conditions are given by:

$$C_1(0,x,y)=C_0 \quad and \quad C_2(0,x,y)=0 \qquad \text{(initial conditions)} \tag{2.19}$$

$$\frac{\partial C_1}{\partial y}=0 \qquad at \qquad y=0 \qquad \text{(symmetry)} \tag{2.20}$$

$$C_1 = C_2, \quad D_1 \frac{\partial C_1}{\partial y} = D_2 \frac{\partial C_2}{\partial y} \quad at \quad y = h \qquad \text{(matching)} \tag{2.21}$$

$$\frac{\partial C_2}{\partial y} = 0 \qquad at \quad y = h_1 \qquad \text{(no flux condition)} \tag{2.22}$$

$$C_1(t, \infty, y) = C_2(t, \infty, y) = 0 \tag{2.23}$$

The above equations are non-dimensionalized using the parameters and neglecting *

$y^* = \frac{y}{h}$, $u^* = \frac{u_i}{u_0}$, $v^* = \frac{v_i}{v_0}$, $\tau^* = \frac{D_1 t}{h^2}$, $\theta_i = \frac{C_i}{C_0}$, $X = \frac{D_1 x}{h^2 u_0}$ we get

Region 1

$$\frac{\partial \theta_1}{\partial \tau} + \phi_1 u_1 \frac{\partial \theta_1}{\partial X} = \chi_i \left(\frac{1}{Pe^2} \frac{\partial^2 \theta_1}{\partial X^2} + \frac{\partial^2 \theta_1}{\partial Y^2} \right) \tag{2.24}$$

Region 2

$$\frac{\partial \theta_2}{\partial \tau} + \phi_2 u_2 \frac{\partial \theta_2}{\partial X} = \chi_i \left(\frac{1}{Pe^2} \frac{\partial^2 \theta_2}{\partial X^2} + \frac{\partial^2 \theta_2}{\partial Y^2} \right) \tag{2.25}$$

Where

$$\phi_1 = \frac{1 + \frac{\Gamma_1}{1 - n\tau}}{1 + \Gamma_1}, \Gamma_1 = \frac{KN_1}{\rho}, Pe^2 = \frac{u_0^2 h^2}{D_1^2}, \phi_2 = \frac{1 + \frac{\Gamma_2}{1 - n\tau}}{1 + \Gamma_2}, \Gamma_2 = \frac{KN_2}{\rho}, \chi_1 = \frac{1}{1 + \Gamma_1}, \chi_2 = \frac{D_2}{D_1} \frac{1}{1 + \Gamma_2}$$

Initial and boundary conditions become

$$\theta_1(0, x, y) = 1 \quad and \quad \theta_2(0, x, y) = 0 \qquad \text{(initial conditions)} \tag{2.26}$$

$$\theta_1 = \theta_2, \quad \frac{\partial \theta_1}{\partial y} = \Lambda_1 \frac{\partial \theta_2}{\partial y} \quad at \quad y = 1, \ \Lambda_1 = \frac{D_2}{D_1} \qquad \text{(matching)} \tag{2.27}$$

$$\frac{\partial \theta_2}{\partial y} = 0 \quad at \quad y = 1 + h', \qquad \text{(no flux condition)} \tag{2.28}$$

$$\theta_1(t, \infty, y) = \theta_2(t, \infty, y) = 0 \tag{2.29}$$

2.1. Dispersion model.

Let us use the generalized dispersion model proposed by Gill and Sankarasubramanian [24] and solve (2.24), (2.25) using the boundary conditions (2.26) to (2.29), obtaining

$$\theta_i \Sigma_{K=0}^{\infty} f_{iK}(\tau, y) \frac{\partial^K \theta_m}{\partial X^K}, \ i = 1, 2 \tag{2.30}$$

Where $\theta_{mi} = \int_{h_{i-1}}^{h_i} \theta_i dY$ is the mean concentration (2.31)

Integrating (24) and (25) w.r.t Y between h_i *and* h_{i-1}, we get

$$\frac{\partial \theta_{mi}}{\partial \tau_i} + \phi_1 \frac{\partial}{\partial X} \int_{h_{i-1}}^{h_i} u_i \theta_i dY = \chi_i \left(\frac{1}{Pe^2} \frac{\partial^2 \theta_{mi}}{\partial X^2} + \left| \frac{\partial \theta_i}{\partial Y} \right|_{h_{i-1}}^{h_i} \right), i = 1, 2 \tag{2.32}$$

Assuming θ to be diffusive in nature, let us introduce the dispersion coefficient into the model as

$$\frac{\partial \theta_{mi}}{\partial \tau_i} = \Sigma_{j=0}^{\infty} K_{ij} \frac{\partial^j \theta_{mi}}{\partial X^j}, \quad j = 1,2 \tag{2.33}$$

We can find the values of K_{ij} by equating the coefficients of $\frac{\partial^j \theta_{mi}}{\partial X^j}$, $j = 0,1,2,....$ as

$$K_{ij}(\tau) = \chi_i \frac{\delta j^2}{Pe^2} + \chi_i \left| \frac{\partial \theta_i}{\partial Y} \right|_{h_{i-1}}^{h_i} - \phi \int_{h_{i-1}}^{h_i} u_i f_{i\,j-1} dY \tag{2.34}$$

where $f_{i\,j-1} = 0$ and δ_{ij} is the Kronecker delta defined as $\delta_{ij} = \begin{cases} 1, & for \;\; i = j \\ 0, & for \;\; i \neq j \end{cases}$

Equation (2.33) can be truncated after the terms K_{12} and K_{22} without causing errors because the higher terms are negligibly small. The resulting model for the mean concentration will be of the form

For region 1

$$\frac{\partial \theta_{m1}}{\partial \tau_1} = K_{10}(\tau_1)\theta_{m_1} + K_{11}(\tau_1)\frac{\partial \theta_{m_1}}{\partial X} + K_{12}(\tau_1)\frac{\partial^2 \theta_{m_1}}{\partial X^2} \tag{2.35}$$

For region 2

$$\frac{\partial \theta_{m_2}}{\partial \tau_2} = K_{20}(\tau_2)\theta_{m_2} + K_{21}(\tau_2)\frac{\partial \theta_{m_2}}{\partial X} + K_{22}(\tau_2)\frac{\partial^2 \theta_{m_2}}{\partial X^2} \tag{2.36}$$

To solve (2.35) and (2.36), we need the values of $K_{ij}\, for\; i,j = 0,1,2$, along with the boundary conditions. To find these values, we require the corresponding values of $f_{ik}\, for\; i = 1,2$. Hence we substitute (2.30) into (2.34) and (2.35) and use (2.32) to get

$$\frac{\partial f_{ik}}{\partial \tau_i} = \chi_i \frac{f_{i,k-2}}{Pe^2} + \chi_i \left(\frac{\partial^2 f_{ik}}{\partial Y^2} \right) - \phi_i u_i f_{ik-1} - \Sigma_{j=0}^{l} K_{i,k-j}, i = 1,2, k = 0,1,2,... \tag{2.37}$$

The initial and boundary conditions required to solve (37) are

$$\theta_{mi} = \int_{h_{i-1}}^{h_i} \theta_i(0, X, Y)\, dY,\; f_{i,k}(0,Y) = 0 \;\; for\; i = 1,2 \tag{2.38}$$

$$\frac{\partial f_{10}}{\partial Y} = 0 \qquad at \qquad Y = 0 \tag{2.39}$$

$$f_{10} = f_{20}, \quad \frac{\partial f_{10}}{\partial Y} = \Lambda \frac{\partial f_{20}}{\partial Y} \qquad at \qquad Y = 1, \tag{2.40}$$

$$\frac{\partial f_{20}}{\partial Y} = 0 \qquad at \qquad Y = 1 + h', \tag{2.41}$$

$$\theta_{mi}(\tau, \infty) = \frac{\partial \theta_{mi}}{\partial X}(\tau, \infty) = 0 \quad for \quad i = 1,2 \tag{2.42}$$

The values of K_{i0} can be obtained from (2.34) as

$$K_{i0} = \chi_i \left| \frac{\partial f_{i0}}{\partial Y} \right|_{h_{i-1}}^{h} \quad for \quad i = 1,2 \tag{2.43}$$

The values of f_{i0} can be obtained from (2.37) as

$$\frac{\partial f_{i0}}{\partial \tau_i} = \chi_i \frac{\partial^2 f_{i0}}{\partial Y^2} - K_{i0} f_{i0} \quad for \quad i = 1,2 \tag{2.44}$$

The solution of (2.44) may be formulated as

$$f_{i0} = \exp\left(-\int_0^{\tau_i} K_{i0}(\eta) d\eta \; g_{i0}(\tau_i, Y) \right) \quad for i = 1,2 \tag{2.45}$$

where g_{i0} must satisfy the following:

$$\frac{\partial g_{i0}}{\partial \tau_i} = \chi_i \frac{\partial^2 g_{i0}}{\partial Y^2} \quad for \;\; i = 1,2 \tag{2.45a}$$

$$f_{10}(0,Y) = g_{10}(0,Y) = \frac{g_{10}(\tau,Y)}{\int_0^1 g_{10}(\tau,Y) dY} \tag{2.45b}$$

$$f_{20}(0,Y) = g_{20}(0,Y) = \frac{g_{20}(\tau,Y)}{\int_1^{1+h'} g_{20}(\tau,Y) dY} \tag{2.45c}$$

$$\frac{\partial g_{10}}{\partial Y} = 0, \qquad at \qquad Y = 0 \tag{2.45d}$$

$$g_{10} = g_{20}, \quad \frac{\partial g_{10}}{\partial Y} = \Lambda \frac{\partial g_{20}}{\partial Y} \quad at \quad Y = 1 \tag{2.45e}$$

$$\frac{\partial g_{20}}{\partial Y} = 0 \qquad at \qquad Y = 1 + h' \tag{2.45f}$$

The solution of (2.45a) using (2.45b) to (2.45f) is obtained as

$$g_{10}(\tau_1, Y) = \Sigma_{n=0}^{\infty} A_{1n} e^{-\xi_{1n}^2 \tau_1} \cos \mu_{1n} Y \tag{2.46a}$$

$$g_{20}(\tau_2, Y) = \Sigma_{n=0}^{\infty} A_{2n} e^{-\xi_{2n}^2 \tau_2} (\cos \mu_{2n} Y + \tan \mu_{1n} (1+h') \sin \mu_{2n} Y) \tag{2.46b}$$

Where μ_{1n}, μ_{2n} are the roots of $-\mu_{1n} \tan \mu_{1n} = \Lambda \mu_{2n} \tan \mu_{2n} h', \quad for \;\; n = 0,1,2,...$ (2.46c)

The expansion coefficients A_{1n} , A_{2n} are given by

$$A_{1n} = \frac{4 \sin \mu_{1n}}{2\mu_{1n}^2 + \mu_{1n} \sin 2\mu_{1n}}, \tag{2.46d}$$

$$A_{2n} = 4s \left(\frac{4 \sin \mu_{2n}(1+h') - \sin \mu_{2n}}{h' + \sin 2\mu_{1n}(1+h') - \sin 2\mu_{2n} - \tan \mu_{2n}(1+h') \cos 2\mu_{2n}(1+h') + \tan \mu_{2n} \cos 2\mu_{2n}}, \right) \tag{2.46e}$$

Using (45) in (44) we get the following values of $f_{ij} and \; K_{ij}$ as

$$f_{10}(\tau_1, Y) = \frac{\Sigma_{n=0}^{\infty} A_{1n} e^{-\xi_{1n}^2 \tau_1} \cos \mu_{1n} Y}{\Sigma_{n=0}^{\infty} \frac{A_{1n}}{\mu_{1n}} e^{-\xi_{1n}^2 \tau_1} \sin \mu_{1n} Y}, \tag{2.47a}$$

$$f_{20}(\tau_2, Y) = \frac{\Sigma_{n=0}^{\infty} A_{2n} e^{-\xi_{2n}^2 \tau_2} \left(\cos \mu_{2n} Y + \tan \mu_{2n} (1+h') \sin \mu_{2n} Y \right)}{\Sigma_{n=0}^{\infty} \frac{A_{2n}}{\mu_{2n}} e^{-\xi_{2n}^2 \tau_2} \left(\sin \mu_{2n}(1+h') - \sin \mu_{2n} + \tan \mu_{2n}(1+h') \left(\cos \mu_{2n} - \cos \mu_{2n}(1+h') \right) \right)}, \tag{2.47b}$$

$$K_{10}(\tau_1) = -\chi_1 \frac{\Sigma_{n=0}^{\infty} A_{1n}\mu_{1n} e^{-\xi_{1n}^2\tau_1} \sin \mu_{1n} Y}{\Sigma_{n=0}^{\infty} \frac{A_{1n}}{\mu_{1n}} e^{-\xi_{1n}^2\tau_1} \sin \mu_{1n} Y}, \quad (2.47c)$$

$$\text{As } \tau_1 \to \infty, \text{ we get } K_{10}(\infty) = -\chi_1 \mu_{10}^2 \quad (2.47d)$$

$$K_{20}(\tau_2) = -\chi_2 \frac{\Sigma_{n=0}^{\infty} A_{2n} e^{-\xi_{2n}^2\tau_2} \left(-\sin \mu_{2n}(1+h') + \sin \mu_{2n} + \tan \mu_{2n}(1+h')\left(-\cos \mu_{2n} + \cos \mu_{2n}(1+h')\right)\right)}{\Sigma_{n=0}^{\infty} \frac{A_{2n}}{\mu_{2n}} e^{-\xi_{2n}^2\tau_2} \left(-\sin \mu_{2n}(1+h') - \sin \mu_{2n} + \tan \mu_{2n}(1+h')\left(-\cos \mu_{2n} + \cos \mu_{2n}(1+h')\right)\right)}, \quad (2.47e)$$

$$\text{As } \tau_2 \to \infty, \text{ we get } K_{20}(\infty) = -\chi_2 \mu_{20}^2 \quad (2.47f)$$

where μ_{10} *and* μ_{20} are the roots of (2.46c).

Now to find the asymptotic values of K_{ik}, we consider the mean velocity of the fluid flow given by (2.45) and (2.46).

Let us inject the solute into the flow for large values of the time. Then the steady-state function $f_{ik}(Y)$ satisfies the equation

For region 1

$$\frac{d^2 f_{1k}}{\partial Y^2} + \mu_{10}^2 f_{1k} = \frac{u_1}{\bar{u}_1}\frac{\phi_1 f_{1k-1}}{\chi_1} - \frac{1}{\chi_1}\Sigma_{j=1}^{k-1} K_{ij} f_{1k-j} + K_{1k} f_{10} \frac{1}{\chi_1}, \quad k = 1, 2, .. \quad (2.48)$$

The boundary conditions required to solve (2.48) are

$$\frac{df_{1k}}{\partial Y} = 0 \quad at \quad Y = 0 \quad (2.49)$$

Using (2.23) and (2.25) we get

$$K_{1k} = \frac{\left.\frac{df_{1k}}{dY}\right|_{Y=1} \cos \mu_{10} + f_{1k}\mu_{10} \sin \mu_{10} - \int_0^1 \left(\frac{u_1}{\bar{u}_1}\frac{\phi_1 f_{1k-1}}{\chi_1} - \frac{f_{1k-2}}{Pe^2} + \frac{1}{\chi_1}\Sigma_{j=1}^{k-1} K_{ij} f_{ik-j} \right) dY}{\int_0^1 \frac{1}{\chi_1} f_{10} \cos \mu_{10} Y dY} \quad (2.50)$$

For region 2

$$\frac{d^2 f_{2k}}{\partial Y^2} + \mu_{20}^2 f_{2k} = \frac{u_2}{\bar{u}_2}\frac{\phi_2 f_{2k-1}}{\chi_2} - \frac{f_{2k-1}}{Pe^2} + \frac{1}{\chi_2}\Sigma_{j=1}^{k-1} K_{ij} f_{2k-j} + K_{2k} f_{20} \frac{1}{\chi_2}, \quad k = 1, 2, .. \quad (2.50a)$$

The boundary conditions required to solve (50a) are

$$\frac{df_{2k}}{\partial Y} = 0 \quad at \quad Y = 1 + h' \quad (2.51)$$

Using (2.23) and (2.25) we get

$$K_{2k}=\frac{-\left.\frac{df_{2k}}{dY}\right|_{Y=1}\cos\mu_{20}+f_{2k}\mu_{20}\sin\mu_{20}(1+h')-f_{2k}\sin\mu_{20}-\int_0^{1+h'}\left(\frac{u_2}{\bar{u}_2}\frac{\phi_2 f_{2k-1}}{\chi_2}-\frac{f_{2k-2}}{Pe^2}+\frac{1}{\chi_2}\Sigma_{j=1}^{k-1}K_{ij}f_{ik-j}\right)\cos\mu_{20}YdY}{\int_0^{1+h'}\frac{1}{\chi_2}f_{20}\cos\mu_{20}YdY} \quad (2.52)$$

Let the solution of (2.48) and (2.51) be formulated as

$$f_{ik}=\Sigma_{j=0}^{\infty}B_{j,ik}\ \cos\mu_{ij}Y \quad for\ \ i=1,2 \quad (2.52a)$$

Then substituting (2.44a) into (2.48) and (2.51), we get

For region 1

$$f_{j,1k}=\frac{1}{\mu_{10}^2-\chi_1\mu_{1j}^2}\left(-\frac{\chi_1}{Pe^2}\Sigma_{j=1}^{\infty}B_{j,k-2}+\Sigma_{j=1}^{\infty}K_{ij}B_{j,k-j}+\left(\frac{1}{2}+\frac{\sin 2\mu_{ij}}{4\mu_{ij}}\right)^{-1}\phi_1\Sigma_{j=1}^{\infty}B_{j,k-j}I(j,l)\right) \quad (2.52b)$$

where $I_1(j,l)=\int_0^1\frac{u_1}{\bar{u}_1}\cos\mu_{1j}Y\cos\mu_{1l}YdY$

$$I_1(j,l)=\frac{RP}{\bar{u}_1}\left[\frac{a_3}{2}\left(\begin{array}{l}\frac{1}{\left(\omega_1^2-\left(\mu_{1j}+\mu_{1l}\right)^2\right)}\left(\omega_1\sin\omega_1\cos(\mu_{1j}+\mu_{1l})-(\mu_{1j}+\mu_{1l})\cos\omega_1\sin\mu_{1j}\right)+\\ \frac{1}{\left(\omega_1^2-\left(\mu_{1j}+\mu_{1l}\right)^2\right)}\left(\omega_1\sin\omega_1\cos(\mu_{1j}-\mu_{1l})-(\mu_{1j}-\mu_{1l})\cos\omega_1\sin\mu_{1j}-\mu_l\right)\end{array}\right)+\right.$$
$$\left.\frac{1}{\left(\omega_1^2-\left(\mu_{1j}{}^2-\mu_{1l}{}^2\right)\right)}\left(\mu_{1j}\sin\mu_{1j}\cos\mu_{1j}-\mu_{1l}\cos\mu_{1l}\sin\mu_l\right)\right], for(j\neq l) \quad (2.53a)$$

$$I_1(j,l)=\frac{RP}{\bar{u}_1}\left[a_3\left(\begin{array}{l}\left(\frac{\sin\omega_1}{2\omega_1}+\frac{1}{\left(2\left(\omega_1^2-4\mu_{1j}^2\right)\right)}\right)\left(\omega_1\sin\omega_1\cos 2\mu_{1j}-2\mu_{1l}\cos\omega_1\sin 2\mu_{1j}\right)-\\ \frac{1}{2\omega_1^2}-\frac{1}{4\omega_1^2\mu_{1j}}\sin 2\mu_{1j}\end{array}\right)\right], for(j=l) \quad (2.53b)$$

For region 2

$$B_{j,2k}=\frac{1}{\mu_{20}^2-\chi_2\mu_{2j}^2}\left(-\frac{\chi_1}{Pe^2}\Sigma_{j=1}^{\infty}B_{j,k-2}+\Sigma_{j=1}^{\infty}K_{ij}B_{j,2k-j}+\phi_2\left(\frac{h'}{2}+\frac{1}{4\mu_{2j}}\left(\sin\mu_{2j}\left(1+h'\right)\right)-\sin\mu_{2j}\right)^{-1}\Sigma_{j=1}^{\infty}B_{j,2k-1}I_2(j,l)\right)$$

(2.53c)

where $I_2(j,l)=\int_0^{1+h'}\frac{u_1}{\bar{u}_1}\cos\mu_{2j}Y\cos\mu_{2l}YdY$

$$I_2(j,l)=\frac{RP}{2\bar{u}_2}\left[\begin{array}{l}\frac{a_2}{\omega_2}\left(\sin\omega_2(1+h')-\sin\omega_2\right)+\frac{a_2}{\left(\omega_2^2-4\mu_{2j}^2\right)}\left(\begin{array}{l}\omega_2\sin\omega_2(1+h')\cos2\mu_{2j}(1+h')-\\2\mu_{2j}\cos\omega_2(1+h')\sin2\mu_{2j}(1+h')-\\\omega_2\sin\left(\omega_2+2\mu_{2j}\right)\end{array}\right)\\-\frac{a_1}{\omega_2}\left(\cos\omega_2(1+h')-\cos\omega_2\right)-\\\frac{a_1}{\left(\omega_2^2-4\mu_{2j}^2\right)}\left(\begin{array}{l}\omega_2\cos\omega_2 2\mu_{2j}(h')\cos2\mu_{2j}(1+h')-\\\omega_2\cos\omega_2\cos2\mu_{2j}+2\mu_{2j}\sin\omega_2\sin2\mu_{2j}\end{array}\right)-\frac{\lambda h'}{\omega_2^2}-\\\frac{\lambda}{2\omega_2^2 4\mu_{2j}}\left(\sin2\mu_{2j}(1+h')-\sin2\mu_{2j}\right)\end{array}\right],\ for(j=l)$$

(2.53d)

$$I_2(j,l)=\frac{RP}{\bar{u}_2}\frac{1}{\left(\mu_{2j}^2-\mu_{2l}^2\right)}\left(\begin{array}{l}\mu_{2j}\sin\mu_{2j}(1+h')\cos\mu_{2l}(1+h')-\\\mu_{2l}\cos\mu_{2j}(1+h')\sin\mu_{2l}(1+h')-\\\mu_{2j}\sin\mu_{2j}\cos\mu_{2l}+\mu_{2l}\cos\mu_{2j}\sin\mu_{2l}\end{array}\right),\ for\left(j\neq l\right) \quad (2.53e)$$

The solution for (2.45) and (2.46) using (2.48) and (2.52) are as follows:

For region 1,

$$\theta_{m_1}=\frac{1}{2}\left(erf\left(\frac{\phi-X_1}{2\sqrt{T}}\right)+erfc\left(\frac{\phi-X_1}{2\sqrt{T}}\right)\right)e^{\xi} \quad (2.54)$$

where $\int_0^{\tau}K_{10}(Z)dZ=K_{10}\tau_1,\ X_1=\xi_1+\int_0^{\tau_1}K_{11}(Z)dZ=\xi_1+K_{11}\tau_1$

$$T=\int_0^{\tau_1}K_{12}(Z)dZ=K_{12}\tau_1.$$

For region 2,

$$\theta_{m_2}=\frac{1}{\sqrt{2T_0}}\exp\left(\tau_0-\frac{X_0^2}{4T_0}\right) \quad (2.55)$$

where

$$\xi_0 = \int_0^{\tau_2} K_{20}(Z)dZ = K_{20}\tau_2, X_0 = \xi_2 + \int_0^{\tau_2} K_{21}(Z)dZ = K_{21}\tau_2,$$

$$T_0 = \int_0^{\tau_2} K_{22}(Z)dZ = K_{22}\tau_2.$$

3. Results and Discussion

An exact analysis of unsteady convective diffusive solute transfer in a channel bounded by a tissue region under the influence of a magnetic field is analyzed using the approach of Sankarasubramanian and Gill [24]. Due to the applied magnetic field, the injected drug convicted and diffused in the blood flow will be directed towards the tissue region. Degradation can occur only after initialization into tissue cells.

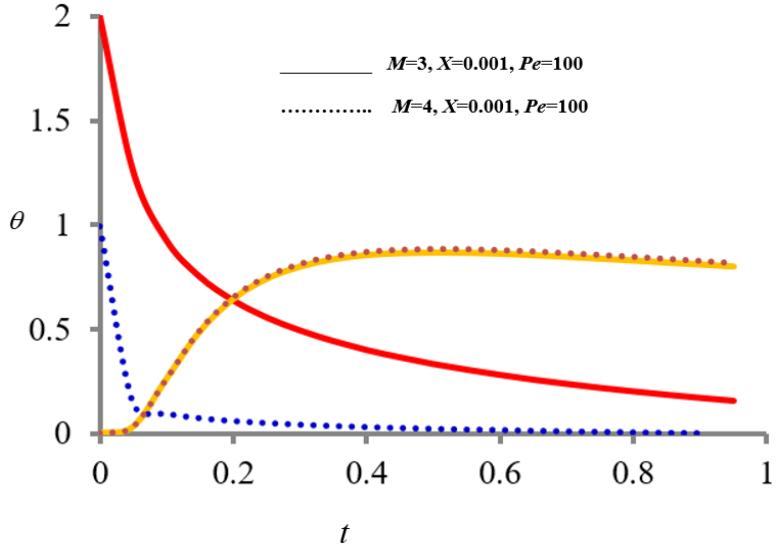

Figure 2. Concentration profile vs. time for different values of magnetic parameter *M*.

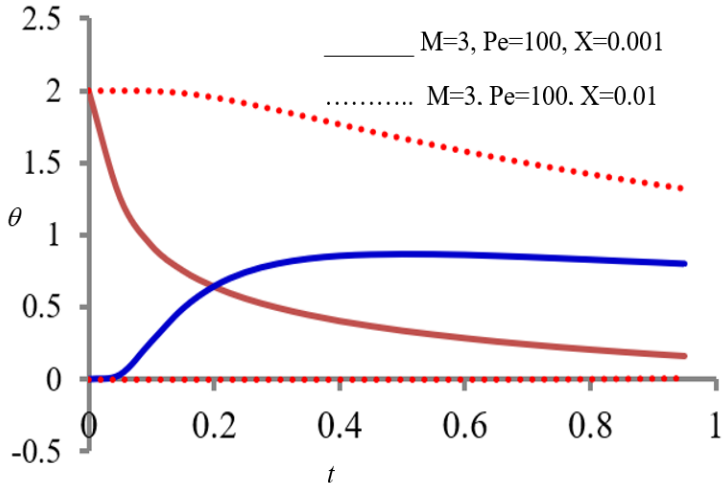

Figure 3. Concentration profile vs time for different values of axial position *X*.

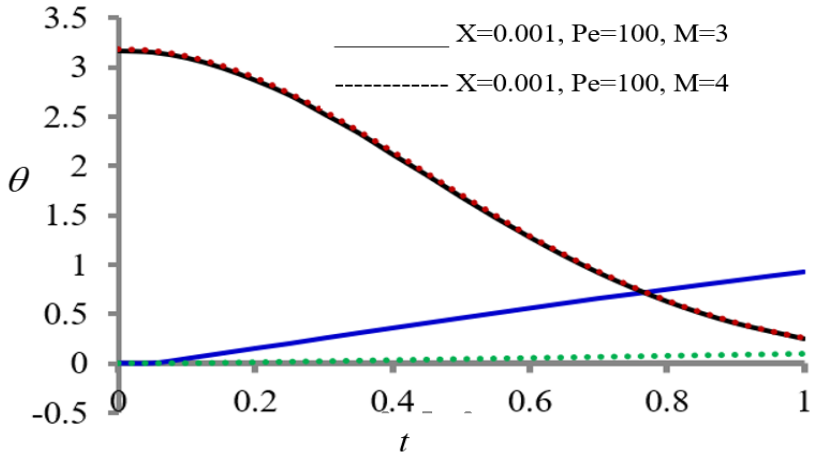

Figure 4. Concentration profile Vs Axial position for different values of magnetic parameter *M*.

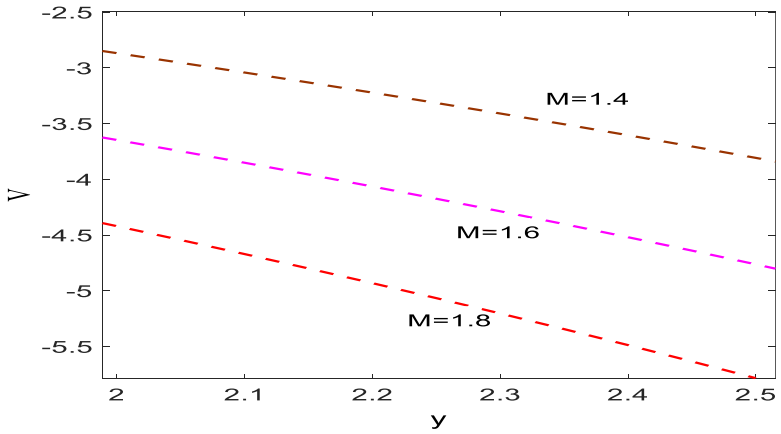

Figure 5. Velocity Profiles in lumen region for different values of magnetic parameter M.

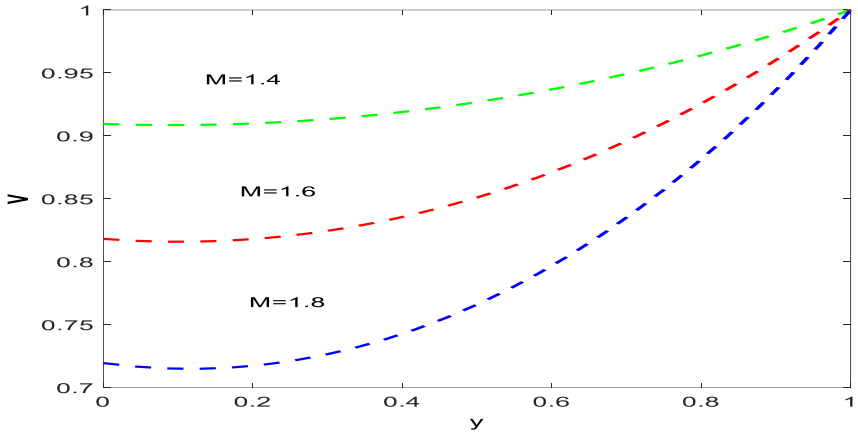

Figure 6. Velocity Profiles in tissue region for different values of magnetic parameter M.

Figures 2-4 show concentration profiles for regions 1 and 2 for different values of magnetic parameter M, Peclet number P_e and axial position X.

Concentration $\theta_1$in lumen decreases with time and θ_2 in the tissue region increases and reaches a constant value. The effect of magnetic field results in a decrease of $\theta_1$in a lesser time, indicating more solute is moving towards the tissue where there is a slight increase of θ_2 in region 2 with an increase in M. The fluid is injected at $X = 0$. The presence of a magnetic field around this region shows dispersion at $X = 0.001$ is at a faster rate than at $X = 0.01$, which is a bit away from the magnetic field.

Figs. 5- 6 show velocity profiles for regions 1 and 2, respectively, for different values of magnetic parameter M. As M increases, the velocity in both regions decreases. As M increases to a higher value, the velocity becomes pulsatile, which can be seen at M=1.8, where there is a negative region for velocity. The magnetic field creates resistance to the flow of the ferrofluid and attracts the target tissue region due to a reduction in velocity.

Using an external magnetic field directs the solute diffusion towards the magnetic field where the drug is supposed to act. This analysis can be used to study targeted drug delivery and similar situations occurring in other applications.

4. Conclusions

A study on the effect of magnetic properties on drug delivery using analytical methods is presented. Suspended nanoparticles carry drugs from the lumen region to the surrounding tissue region. This is modeled by considering a dusty viscous fluid. A dispersion model proposed by Sankarasubramanian and Gill [24] is modified to account for mass transfer. Pulsatile flow is caused by the magnetic field and affects mass transfer. According to the graphs, the mass transfer will increase from the lumen region to the tissue region. Magnetic parameter and Peclet number are the parameters that significantly affect carrying drugs toward the tissue.

Funding

This research received no external funding.

Acknowledgments

The authors are grateful to the research Center Atria Institute of Technology, REVA University, and Vellore Institute of Technology for their support and encouragement in carrying out our research work.

Conflicts of Interest

The authors declare no conflict of interest.

References

1. Handan L. Process modeling of ferro fluids flow for magnetic targeting drug delivery. *Chin J Mech Eng.* **2009**, *22*, 440, https://doi.org/10.3901/cjme.2009.03.440.
2. Sarkar, A.; Jayaraman, G. The effect of wall absorption on dispersion in annular flows. *Acta Mech.* **2002**, *158*,105–119, https://doi.org/10.1007/bf01463173.
3. Sankarasubramanian, R.; Gill, W.N. Unsteady convective diffusion with interphase mass transfer. *Proc Roy Soc Lond A.* 1973,*333*,115-132, https://doi.org/10.1098/rspa.1973.0051.
4. Mazumder, B.S.; Das, S.K. Effect of boundary reaction on solute dispersion in pulsatile flow through tube. *J Fluid Mech.* **1992**, *239*, 523-549, https://doi.org/10.1017/s002211209200452x.
5. Chamkha, A.J.; Khaled, A.A. A Hydro magnetic combined heat and mass transfer by natural convection from a permeable surface embedded in a fluid saturated porous medium. *Int J Num Methods Heat Fluid Flow.* **2000**, *10*, 455 – 476, https://doi.org/10.1108/09615530010338097.
6. Anderson, D.A.; Tannehill, J.C.; Pletcher, R.H. Computational fluid mechanics and heat transfer. *Hemisphere*. **1984**, 599.
7. Mukherjee, M.; Mazumder, B.S. Dispersion of contaminant in oscillatory flows. *Acta Mech* **1988**, *74*, 107–122, https://doi.org/10.1007/bf01194345.
8. Taylor, G.I. Diffusion by continuous movements. *Proc Roy Soc Lond.* **1921**, *20*,196–211, https://londmathsoc.onlinelibrary.wiley.com/doi/10.1112/plms/s2-20.1.196.
9. Taylor, G.I. Dispersion of solute matter in solvent flowing slowly through a tube. *Proc Roy Soc Lond A.* **1953**, *219*, 186–203, https://doi.org/10.1098/rspa.1953.0139.

10. Yun-dong, T.; Tao Jin, Rodolfo. C.C.F. Effect of mass transfer and diffusion of nanofluid on the thermal ablation of malignant cells during magnetic hyperthermia. *Appl Math Model.* **2020**, *83*,122-135, https://doi.org/10.1016/j.apm.2020.02.010.
11. Sharifi, A.; Yekani, M.S.; Badfar, H. Numerical investigation of magnetic drug targeting using magnetic nanoparticles to the aneurysmal vessel. *J Magn Magn Mater*. **2019**, *474*, 236-245, https://doi.org/10.1016/j.jmmm.2018.10.147.
12. Rahmat E.; Sadiq, M.S.; Shehzad, S.; Mobin, N. Numerical simulation and mathematical modeling of electro-osmotic Couette–Poiseuille flow of MHD power-law nano fluid with entropy generation. *Symmetry*. **2019**, *11*, 1038, https://doi.org/10.3390/sym11081038.
13. Varmazyar, M.; MohammadReza, H.; Meysam, A.; Ahmad H. P.; Masoud A.; Seyed, M.V. Numerical simulation of magnetic nanoparticle-based drug delivery in presence of atherosclerotic plaques and under the effects of magnetic field. *Powder Techn.* **2020**, *366*, 164-174, https://doi.org/10.1016/j.powtec.2020.02.009.
14. Nadeem, S.; Adel, A.; Noor, M.; Ibrahim, M.A.; Alibek, I.; Mustafa, M.T. A computational model for suspensions of motile micro-organisms in the flow of ferrofluid. *J Mol Liq.* **2020**, *298*,112033, https://doi.org/10.1016/j.molliq.2019.112033.
15. Punith Kumar, D.; Indira, R.; Sravan Kumar, T. MHD on convective mass transfer in annular flow: catheter-based drug release. *Biointerface Res Appl Chem.* **2021**, *12*, 6699-6709, https://doi.org/10.33263/briac125.66996709.
16. Ismaeel, A.M.; Mansour, M.A.; Ibrahim, F.S.; Hady, F.M. Numerical simulation for nanofluid extravasation from a vertical segment of a cylindrical vessel into the surrounding tissue at the microscale. *Appl Math Comput*. **2022**, *417*, 126758, https://doi.org/10.1016/j.amc.2021.126758.
17. Ghulam, R.; Anum, S.; Marei, S.A.; Abderrahim, W.; Ilyas, K.; Muhammad, S.B. Numerical scrutinization of Darcy-Forchheimer relation in convective magnetohydrodynamic nanofluid flow bounded by nonlinear stretching surface in the perspective of heat and mass transfer. *Micromachine.* **2021**, *12*, 374, https://doi.org/10.1016/j.amc.2021.126758.
18. Farshad, M.k.; Soltani, M.; Mohammad, M.M.; Arman, R. Enhanced drug delivery to solid tumors via drug-loaded nanocarriers: An image-based computational framework. *Frontiers in Oncology*. **2021**, *11*, 1-19, https://doi.org/10.3389/fonc.2021.655781.
19. Sahai, N.; Gogoi, M.; Ahmad, N. Mathematical modeling and simulations for developing nanoparticle-based cancer drug delivery systems: a review. *Current Pathobiology Reports.* **2021**, *9*, 1-8, https://doi.org/10.1007/s40139-020-00219-5.
20. Punith Kumar, D.N.; Indira, R. Effect of rotation on convective diffusive mass transfer in a magnetically conducting fluid. *Int J Innov Sci Math.* **2017**, *5*, 2347-9051, http://ijism.org/administrator/components/com_jresearch/files/publications/IJISM_659_FINAL.pdf.
21. Zakaria, K.; Smail, B.; Farid, B.; Abdelkader, F. MHD mixed convection and irreversibility analysis of hybrid nanofluids in a partially heated lid-driven cavity chamfered from the bottom side. *Int Commun Heat Mass Transf.* **2022**, *132*, 105895, https://doi.org/10.1016/j.icheatmasstransfer.2022.105895.
22. Xue-LinGao, JianWu, KangLuo, Hong-Liang Yi, He-Ping, T. Lattice Boltzmann analysis of conjugate heat transfer in the presence of electrohydrodynamic flow. *Int Commun Heat Mass Transf.* **2022**, *132*,105878, https://doi.org/10.1016/j.icheatmasstransfer.2021.105878.
23. Sukumar, P.; Abhijit, B.; Manash, P.; Boruah, P.; Randive, R. Critical review on local thermal equilibrium and local thermal non-equilibrium approaches for the analysis of forced convective flow through porous media. *Int Commun Heat Mass Transf.* **2022,** *132*, 105889, https://doi.org/10.1016/j.icheatmasstransfer**.2022.1**05889.
24. Sankarasubramanian, R.; Gill, W.N. Unsteady convective diffusion with interphase mass transfer. *Proc Roy Soc Lond.* **1973**, *333*, 115-132, https://doi.org/10.1098/rspa.1973.0051.
25. Sravan Kumar, T.; Punith Kumar, D.N.; Sreevallabha Reddy, A. Study of mixed convective–radiative fluid flow in a channel with temperature-dependent thermal conductivity. *Partial Differ Equ Appl Math*. **2022**, 5, 100344, https://doi.org/10.1016/j.padiff.2022.100344.
26. Sravan Kumar, T.; Dinesh, P.A.; Suresh Babu, R.; Sreevallabha Reddy, A. Numerical study of moving fin with thermal properties. *Heat Transf.* **2022**, 51, 5623-5634, https://doi.org/10.1002/htj.22562.
27. Sravan Kumar, T. Hybrid nanofluid slip flow and heat transfer over a stretching surface. *Partial Differ Equ Appl Math*. **2021**, 4, 100070, https://doi.org/10.1016/j.padiff.2021.100070.
28. Suresh Babu, R.; Ramesh, N.L.; Sravan Kumar T. Effects of chemical reaction, Soret and Lorentz force on Casson fluid flow past an exponentially accelerated vertical plate: A comprehensive analysis. *Heat Transf.* **2022**, 51, 2237- 2257, https://doi.org/10.1002/htj.22398.
29. Nilankush, A.; Chamkha, A.J. On the magnetohydrodynamic Al2O3-water nanofluid flow through parallel fins enclosed inside a partially heated hexagonal cavity. *Int Commun Heat Mass Transf*. **2022**, *132*,105885, https://doi.org/10.1016/j.icheatmasstransfer.2022.105885.